JOURNAL OF GEOPHYSICAL RESEARCH, VOL. 102, NO. E7, PAGES 16,327–16,338, JULY 25, 1997

Gradation of the Roter Kamm impact crater, Namibia

John A. Grant,[1] Christian Koeberl,[2] Wolf Uwe Reimold,[3] and Peter H. Schultz[4]

Abstract. Interpretation of ground penetrating radar data from the 3.7 Ma old Roter Kamm impact crater, together with results of petrographic and sedimentologic analysis of sediment samples, indicates that ~40 m or more of slope sensitive degradation of the rim was accompanied by reduction of wall slopes well below the angle of repose and nearly complete erosion of ejecta from around the crater. Only one patch of in situ ejecta deposit was identified. Degradation of both the interior and exterior of the crater was dominated by fluvial/alluvial activity, likely during the first 1.0-2.7 Ma history of the crater. Eolian modification has dominated gradation since the last half of the Pleistocene. Results from Roter Kamm can help in evaluating evolution of degraded Martian craters that may have experienced fluvial/alluvial gradation followed by eolian modification. On Mars, extended fluvial/alluvial activity should produce a low sloped, incised rim, thereby eroding most of the continuous ejecta well before removal of easily recognizable rim relief. Subsequent eolian deposition can bury all but the raised rim of craters, thereby creating a focal point for efforts geared towards constraint of gradational history.

Introduction

The Roter Kamm crater is located in the southern Namib desert, Namibia (27°46'S; 16°18'E, Figure 1), and was formed approximately 3.7 m.y. ago [*Koeberl et al.*, 1993]. An impact origin for the crater was proposed [*Dietz*, 1965; *Fudali*, 1973] and then confirmed [*Miller and Reimold*, 1986; *Reimold and Miller*, 1989; *Reimold et al.*, 1988, 1994] on the basis of morphologic, geophysical, petrologic, and geochemical evidence. Evaluation of the preservation state of the simple crater and any associated ejecta, however, has been hindered by the remote location and its almost complete burial by an active regional sand sheet [*Miller and Schalk*, 1980; *McKee*, 1982].

In an attempt to resolve the degradation history of the crater, an expedition was undertaken in 1995 to deploy a ground penetrating radar instrument (GPR) and map the present expression of the crater beneath the sand sheet. The primary goal was to define the characteristics and extent of any continuous ejecta preserved beyond the crater rim.

Geologic Setting and Crater Description

At present, Roter Kamm is approximately 2.5 km in diameter (rim crest to rim crest) and possesses a rim reaching between 40 and 90 m above the surrounding plain. Local rim relief is significant and varies by as much as 30 m over distances of as little as 0.5 km along the southerly quarter (Plate 1). Sands associated with a regional deposit bury all but the highest portions of the rim and are frequently shaped into longitudinal dunes with a relief of 5-10 m. Dunes are best developed east and west of the crater where they are oriented generally southeast-northwest.

Eolian infilling of up to 500 m [*Fudali*, 1973] limits the present maximum depth of the crater to ~50 m below the level of the surrounding plain. Interior sands thin toward the rim crest, where bedrock and alluvial/colluvial debris are exposed. Topographic profiles completed during this study (Plate 1) indicate gradients on the exposed bedrock and alluvium-mantled interior walls are well below the repose angle of 30°-35° expected for unconsolidated debris [*Ritter et al.*, 1995]: the steepest sections range between 17° and 22° from the horizontal, are located to the east northeast, and correlate with areas of maximum rim height. Lowest slopes are only 8°-10°, occur to the south, and correlate with areas of minimum rim height (Plate 1).

Mobile sediments associated with the regional sand sheet are 0-10 m thick around the outside of the crater and cap a relatively simple stratigraphic sequence. Outcrops along an erosional escarpment north-northeast of the crater together with sample pits reveal pedogenic calcrete generally of stage III, IV, and higher (nodular to lamellar to massive [after *Gile et al.*, 1966; *Machette*, 1985]) at the base of the sands. Upward migration of calcrete fragments in areas where the sand cover is only 1-2 m in thickness creates a patchy, very low density pavement. Depending on location, units beneath the sand sheet and calcrete include paleodune sediments, older calcrete horizons, and/or bedrock. Bedrock in the vicinity of the crater consists of a discontinuous cover of Gariep metasediments above Precambrian granitic and granodioritic orthogneisses [*Miller and Schalk*, 1980; *Reimold and Miller*, 1989; *Reimold et al.*, 1994; *Koeberl et al.*, 1993]. Lithologies noted in outcrops along the crater rim and fragments recovered from beneath sands burying the crater flank and exterior are overwhelmingly granitic and granodioritic orthogneisses.

Although the crater is well preserved from a structural standpoint, the state of secondorder morphology, specifically the character and extent of any continuous ejecta deposit, was largely unconstrained. Such uncertainties reflect both the limited research due to the remote location of the crater within

[1]Earth Sciences, State University of New York College at Buffalo.
[2]Institute of Geochemistry, University of Vienna, Vienna, Austria.
[3]Department of Geology, University of Witwatersrand, Johannesburg, South Africa.
[4]Geological Sciences, Brown University, Providence, Rhode Island.

Paper number 97JE01315.
0148-0227/97/97JE-01315$09.00

Figure 1. Landsat thematic mapper (TM) view of the Roter Kamm impact crater and vicinity, Namibia (centered at 27°46'S; 16°18'E). Black lines mark the location of GPR transects completed in and around the crater. Transects shown are longer than 100 m: numerous shorter transects were completed within and outside of the crater but are not displayed. Image resolution is 30 m/pixel.

the restricted access diamond "Sperrgebiet" as well as the extensive cover created by the sand sheet. Hence attempts to investigate the gradation history of the crater and any associated ejecta involve remote and/or physical penetration through the sand cover.

GPR and the Present Study

An approach combining GPR deployment with excavation and field sampling was used to probe beneath the sand sheet at the crater. GPR is a proven instrument in arid impact environments [*Pilon et al.*, 1991; *Grant and Schultz*, 1993a,

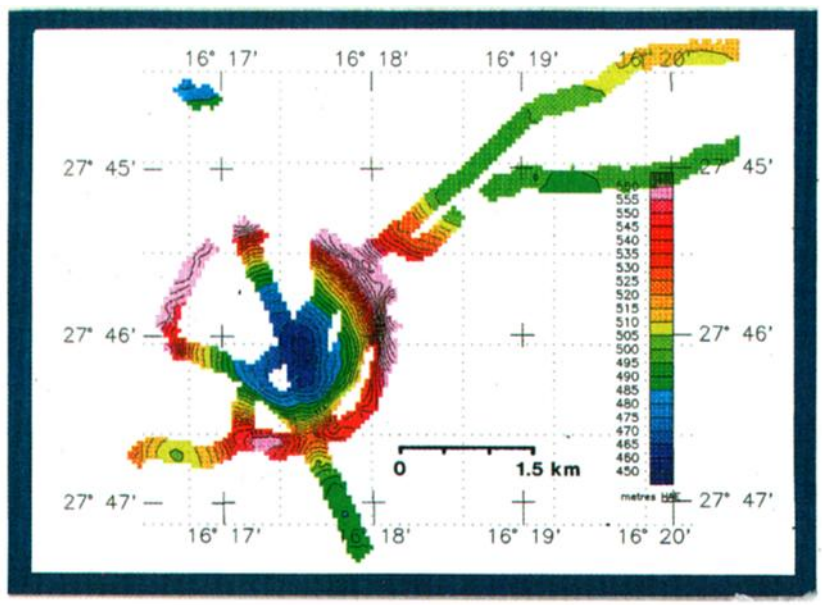

Plate 1. Topography associated with the Roter Kamm impact crater. Data collected using mobile GPS in conjunction with fixed base station established in town of Bethanie, Namibia, located ~150 km to the northeast of the crater (field differential measurements). Contour interval is 5 m, and north is toward the top. Data were collected using a sample spacing of ~30 m on high relief portions of the rim flank and interior wall (wherever possible) and at somewhat lower spatial resolution (~100 m) on the lower relief plains surrounding the crater.

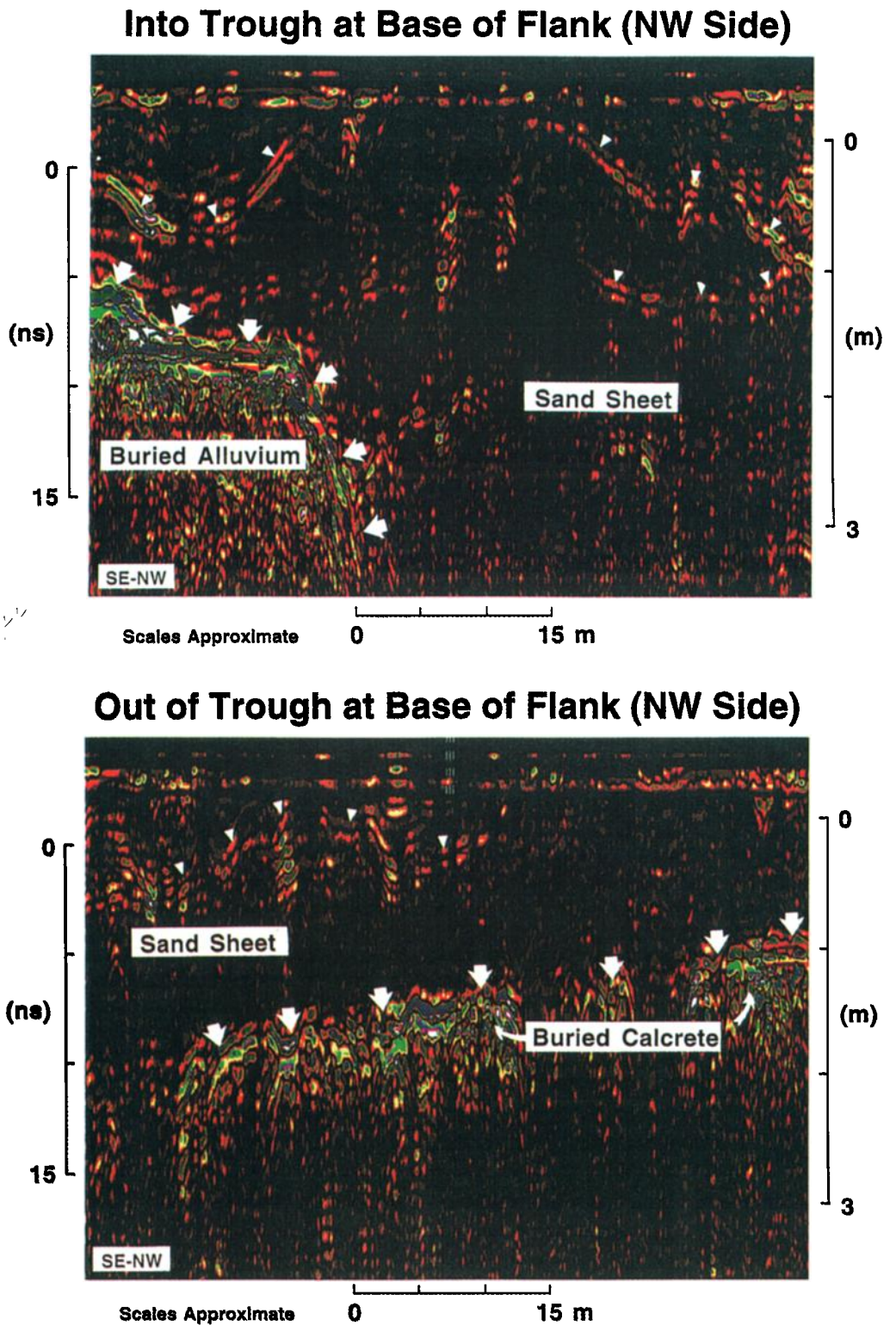

Plate 2. GPR transects (a) toward the bottom of the northern flank of the crater and into the swale and (b) coming out of the swale heading away from the crater. Both transects were completed using a 500 MHz transducer and data were filtered and migrated to restore local relief: data migration in Plate 2a did not include restoring the general decrease in elevation down the flank. The small white arrowheads in both Plates 2a and 2b correspond to reactivation surfaces within the eolian sand sheet filling the swale and burying flanking surfaces (see also Figure 3). The reflection on the crater flank (Plate 2a) highlighted by the white arrows corresponds to the upper surface of a deposit of sorted and rounded fragments derived from higher along the rim. By contrast, white arrows define a reflection rising out of the swale (Plate 2b) that corresponds to the surface of an extensive calcrete layer located beneath the sand sheet on the surrounding plains. Direct sampling and tracing to outcrop reveals that the calcrete here and elsewhere directly overlies paleodune deposits and/or bedrock: ejecta are not present within or beneath the calcrete.

1994a; *Grant et al.*, 1996] and provides an effective tool for defining dielectric contrasts in the shallow subsurface that often correspond to changing stratigraphy and/or structure (e.g., *Ulriksen*, 1982; *Doolittle*, 1987; *Olhoeft*, 1988; *Grant and Schultz*, 1994a]. Moreover, relative portability of the instrument permits deployment along transects ranging from meters to kilometers in length, and resultant data help to pinpoint locations where excavation of sample pits for ground truth provide maximum information on subsurface properties.

Results of GPR analyses at Roter Kamm during a recent expedition (1995) to the crater and subsequent evaluation of sedimentologic data are considered in the context of topographic position to define units whose depositional record can be used to evaluate past gradational activity. Next, the character and extent of these units are used to place preliminary constraints on processes responsible for gradation. Finally, the possible implications of our results for interpreting the evolution of some degraded Martian craters are discussed.

Experimental Methods

Investigations with the GPR at Roter Kamm were geared toward delineation of units preserved beneath the regional sand sheet. Operation in a continuous mode permitted the character and extent of the defined units to be evaluated over distances that were precluded by direct sampling. In addition, GPR data were used to pinpoint locations where excavation and sampling could provide maximum information regarding the sedimentology and stratigraphy of buried surfaces/units.

The strategy for using the GPR was based on assessment of air photos and satellite imagery of the crater (e.g., Figure 1). Initial transect locations were located on the basis of general surface character (e.g., local high versus low relief), position and relief of dune fields, proximity to outcrops (e.g., along the rim and along an erosional escarpment NE of the crater), and the desire to characterize as much of the crater as possible during limited time in the field. The original deployment and sampling strategy was modified as warranted by the accessibility of targeted areas (e.g., some high relief sections of the rim and the region to the west of the crater were not investigated) and as a result of preliminary data analysis in the field. Deployment was from the north side of the crater clockwise towards the south along radial and circumferential transects ranging from 50 m to over 5 km in length. Transects totaled ~15 km in length and targeted the interior wall of the crater, exposed rim areas, and the outer flank and surrounding plains (Figure 1).

The GPR work involved a fully digital Geophysical Survey Systems, Inc. (GSSI), SIR-10a system configured with both a monostatic 500 MHz transducer (60 cm wavelength) and bistatic 100 MHz transducer (3 m wavelength). The 500 MHz transducer enables definition of objects whose dimensions approach the wavelength of the radar pulse (tens of centimeters) and returns are dominated by reflections from objects located directly below the transducer. The 100 MHz

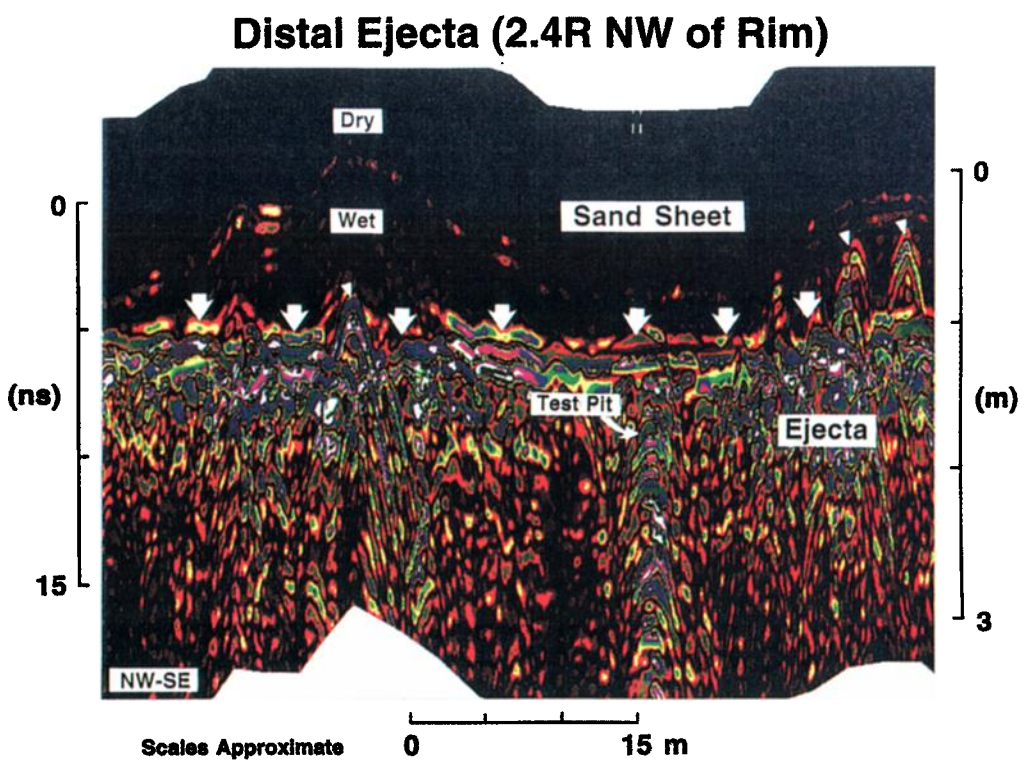

Plate 3. GPR transect across a slightly elevated surface 2.4 crater radii northwest of the rim defining a prominent reflection (marked by white arrows). Sampling and burial of target reflectors confirm the relatively blocky, poorly sorted, subangular character of the deposit as compared to the crater flank alluvium deposits. Individual blocks that have migrated slightly above the surrounding deposit are marked by smaller white arrowheads. The relatively continuous reflection near the top (especially visible on the left side of the figure) marks the transition from dry surface sands to deeper, damper sands of the eolian sand sheet (see Figure 3). Data were collected with a 500 MHz transducer and were filtered and migrated to restore local relief.

transducer typically provides greater penetration and resultant data are capable of resolving objects ~1-2 m in size. It is important to note that definition of subsurface units at Roter Kamm was based on the general radar character as defined over distances of tens of meters and was validated via sampling.

Data were recorded on an Exabyte tape drive to permit subsequent transfer to a lab system where processing, which included additional horizontal filtering and data migration, was accomplished using GSSI RADAN3 software. Confirmation of the position and character of reflections identified in the data involved excavation of sample pits at locations selected from review of the GPR data, burial of target reflectors along the transect lines, and/or tracing the reflectors to outcrop.

Definition of the depositional environment of the units delineated using the GPR involved evaluation of several sedimentologic parameters together with consideration of topographic position. Textural and stratigraphic properties of depositional sequences are often used as an aid in distinguishing processes responsible for their origin [e.g., *Matthews*, 1974; *Folk*, 1980; *Leeder*, 1982; *Scholle and Spearing*, 1982]. These properties include grain size, grain shape, and degree of sorting, the occurrence and scale of bedding and/or internal structure/stratification, and the relative geometry of the deposits. Difficulties can arise in distinguishing the process(es) responsible for the origin some deposits, however, when texturally uniform sources are made available for erosion and transport. Texturally uniform sources may be created by intergranular disintegration (e.g., sandstone and equigranular granite) or exposure of facies possessing a narrow range in grain properties (e.g., loess). Hence resultant deposits can be difficult to distinguish regardless of the process responsible for their formation. Moreover, thresholds controlling the rate and intensity of gradation are influenced by factors including climate, lithology, and structure [*Scholle and Spearing*, 1982; *Ritter et al.*, 1995]. As a result, differing processes can create depositional units whose range in sedimentologic and stratigraphic properties overlap. For example, distinction between some glacial and other mass wasting deposits can be difficult, especially when based solely on the textural properties and local stratigraphic character.

The gradational system is simplified at Roter Kamm, however, because crater topography punctuates an otherwise low relief plain and the relatively dry, non-glacial climate over the past 3.7 m.y. [*Cooperative Holocene Mapping Project (COHMAP)*, 1988; *deMenocal*, 1995] limits the number and intensity of processes contributing to gradation. Potential processes include mass wasting, fluvial/alluvial activity (including slope wash), and eolian deflation/deposition. Lacustrine processes may have been active on the floor of the crater during wetter-than-present conditions [e.g., *deMenocal*, 1995], but any evidence of such activity lies deeply buried beneath the eolian crater fill. However, there is evidence in the crater rim rocks that a postimpact hydrothermal system was active at least for a short time after the impact event [*Koeberl et al.*, 1989; *Reimold et al.*, 1994].

Impact events producing simple craters larger than ~1 km in diameter typically result in partial to complete comminution of bedrock and excavation of angular, poorly sorted fragments covering a wide range in grain size [e.g., *Shoemaker*, 1960; *Shoemaker and Kieffer*, 1974; *Grant and Schultz*, 1993a]. Much of the comminuted and excavated material is derived from below any near-surface weathering zones. The complex structure at Roter Kamm further increases the expectation that the excavated material will comprise a range of grain sizes. Direct observations confirm that subsequent weathering of partially comminuted or fractured bedrock now exposed along the crater rim produce fragments ranging from individual crystal grains to blocks of granitoid basement exceeding 1 m in diameter.

At Roter Kamm the combination of geologic and climatic setting together with the availability of widely varying grain sizes for erosion and transport should result in deposits of distinguishable character. For example, comparisons of the

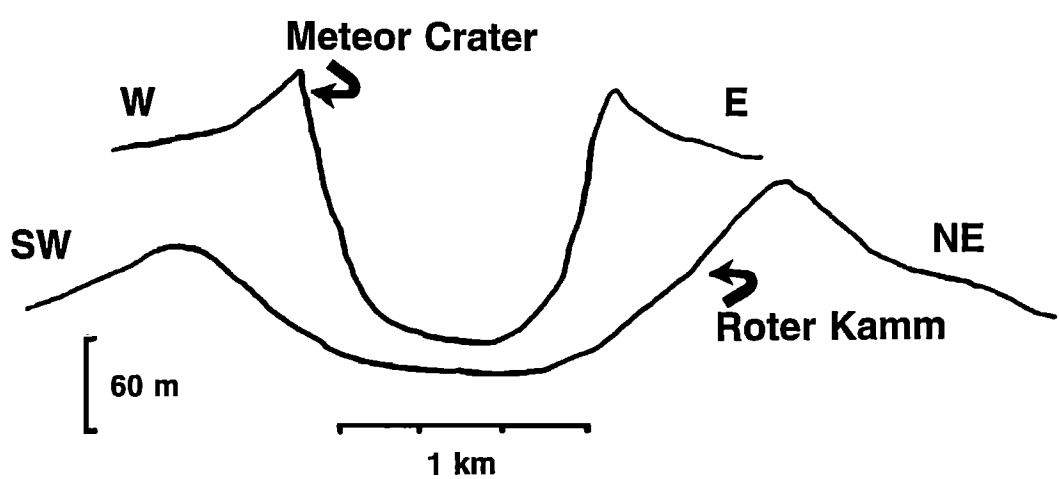

Figure 2. Topographic profiles for the ~2.5 km diameter Roter Kamm (3.7 m.y. old) and the ~1.2 km diameter Meteor Crater in Arizona (50,000 years old). The profile of the rim portion of Roter Kamm is substantially rounded relative to the fairly pristine Meteor Crater (even after accounting for differences in the size of the craters). Note that the slope of the interior wall at Roter Kamm is fairly uniform for at least 500 m from the rim, thereby suggesting that the gradients on surfaces beneath the upper edge of the eolian crater fill (see text for discussion) persist beyond the limit of the GPR transects. The profile for Roter Kamm crosses the crater from SW to NE and was completed using data presented in Plate 1. The profile for Meteor Crater is from W to E and was completed using published U.S. Geological Survey topographic maps. Profiles for both craters are displayed at the same scale and are drawn using a 6:1 vertical exaggeration.

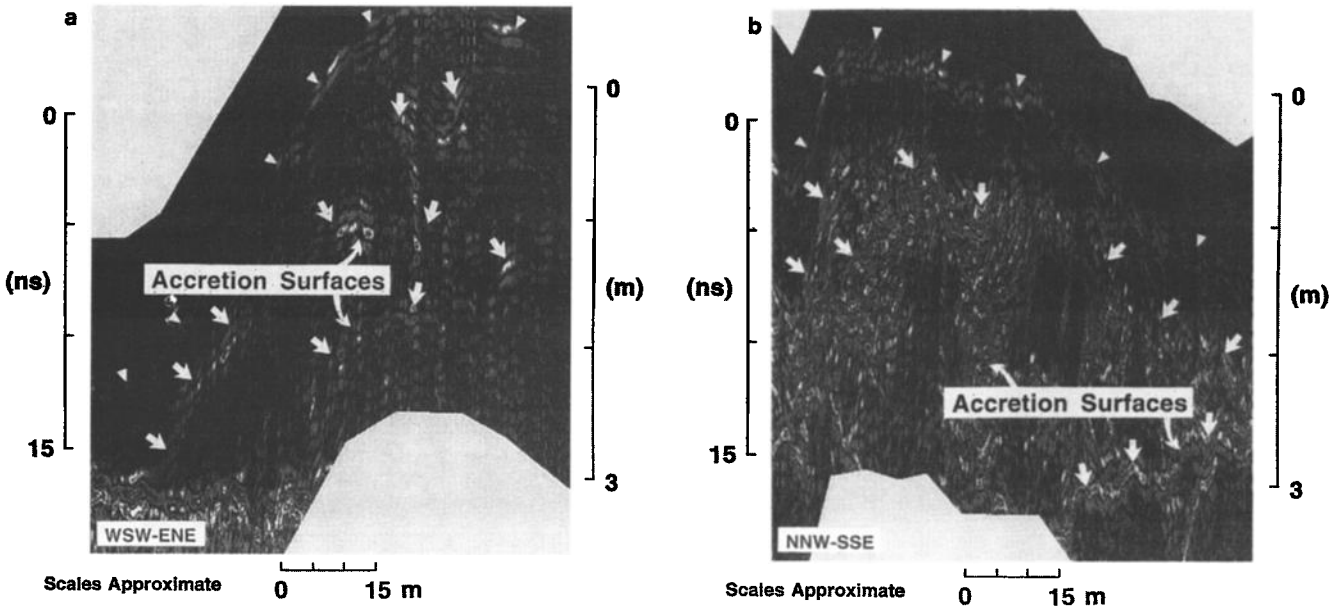

Figure 3. GPR transects through dunes (a) east and (b) south of Roter Kamm. The fairly continuous reflection (small white arrowheads) in both Figures 3a and 3b mark the position of a wetting front in the sands and is discernible in many of the subsequent figures. Data in both Figures 3a and 3b were collected using a 500 MHz transducer and were filtered and migrated to restore topography. Deeper reflections in both figures mark the position of accretion/reactivation surfaces (white arrows). The stacked appearance of such reflections in Figure 3a highlights the relatively stable position of dunes east of the crater, whereas the chaotic appearance of the reflections from south of the crater reflects less positional stability due to the disruption of prevailing winds by rim topography. The more prominent reflection in the lower left corner of Figure 3a is described in Plate 2a.

textural properties of deposits resulting from mass wasting/colluvial versus fluvial/alluvial versus eolian should reveal trends that include decreasing modal grain size, increasing sorting, and increasing grain rounding. Comparable trends related to topographic position and stratigraphic character should also be definable. Collectively, these textural properties and topographic and stratigraphic characteristics serve as the criteria for definition of depositional units at Roter Kamm and for identification of processes responsible for their origin. A similar approach was successful in defining the origin of depositional units at Meteor Crater, Arizona [*Grant and Schultz*, 1993a, b; 1994a, b], where aspects of the topographic, geologic, and climatic setting that influence slope sensitive gradation are similar to those at Roter Kamm.

Samples obtained from around the crater were analyzed on the basis of topographic position, stratigraphy noted in outcrop and GPR data, and information related to grain size, sorting, and shape. Grain analysis was completed using standard methods described by *Matthews* [1974] and *Folk* [1980]. Sieve analyses of grain size were completed at 1/2 phi increments (phi units = mm $-\log_2$) and some samples were washed in a ~2 N HCl solution prior to analysis to dissolve pedogenic calcrete precipitates binding some granitic and granodioritic fragments. Cursory evaluation of the samples prior to dissolution revealed a paucity of non-pedogenic carbonate fragments and cements. The degree of grain sorting is based on the standard deviation of the grain size and is reported using the classification presented by *Matthews* [1974]. Definition of grain shape involved comparative, qualitative assessment of the degree of grain rounding in samples obtained from beneath the regional sand sheet.

Data and Interpretation

Topographic data collected at Roter Kamm provide the first clues regarding the preservation state of the crater (Plate 1 and Figure 2). By way of comparison with the relatively young (50,000 years old [*Sutton*, 1985]) and pristine Meteor Crater [*Grant and Schultz*, 1993a], Roter Kamm (which is about 75 times older) presents a subdued form. Gradients on surfaces within Roter Kamm are significantly below the angle of repose, and the rim crest region is relatively broader and more rounded than at Meteor Crater (Figure 2). The broader rounded form of the rim at Roter Kamm persists around the crater (Plate 1) and reflects significantly less short wavelength topographic variability relative to Meteor Crater.

Examination of the GPR data from Roter Kamm permits identification of a variety of reflections to depths of up to 3-5 m that provide additional information regarding preservation state. Penetration of the GPR signal is sufficient to probe through the regional sand sheet and into underlying units in almost all locations beyond the rim that were evaluated. As such, the radar data effectively create a window through the sand sheet and permits older underlying surfaces and morphology to be delineated.

Excavation in and through the sand sheet covering the crater flank and subsequent analysis of samples constrain the dielectric properties and sedimentology of near-surface stratigraphy and assist in determining the origin of the units defined by the GPR reflections. Pulse travel times in the sand sheet are 16-17 cm/ns and correspond to a dielectric constant of 3.3-3.6. Sediment comprising the sand sheet are moderately sorted (standard deviation of multiple grain size analyses is 0.875 phi units), possess a modal grain size of 0.20-0.25 mm,

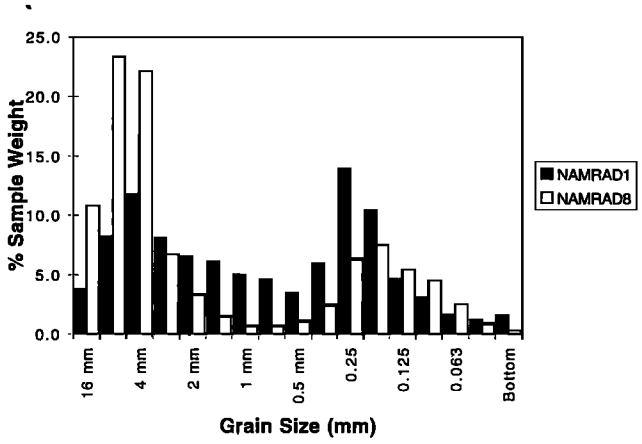

Figure 4. Grain size histogram of the sediment comprising the crater flank deposit described in Plate 2a. Sediment was sieved at 1/2 phi intervals (denotes grain size in mm $-\log_2$) and demonstrates the deposit is coarser (mode at 4-8 mm) than local eolian sediments (represented by the finer mode at 0.20-0.25 mm created by inclusion of eolian sediments that slumped into the sample pit during excavation). The degree of sorting (standard deviation in grain size ranges between 1.1 and 1.6 phi units) and rounded character of fragments in the deposit are most consistent with an origin related to fluvial transport and alluvial deposition. Sample was not washed in HCl solution prior to sieving because pedogenic carbonate accumulations are less developed on the well-drained crater flank.

and are similar to eolian sediments elsewhere [e.g., *McKee*, 1982; *Grant and Schultz*, 1993a]. GPR data from within the sand sheet commonly delineate a reflection at depths of 0.5 to 1.0 m that mirrors surface topography (Figures 3a and 3b). Deeper reflections from within the longitudinal dunes north and east of the crater form stacked sequences (Figure 3a), whereas reflections in dunes south of the rim are more chaotic (Figure 3b). Excavations revealed that the shallower reflection correlates with a transition from dry to damp sand, whereas the deeper reflections mark the location of reactivation/accretion surfaces within the dunes. Detection of the shallow reflection highlights the sensitivity of the GPR to variations in subsurface moisture, while detection of the deeper reactivation surfaces reveals the relative stability of dune positions (Figure 3a) with the exception of locations where crater rim topography disrupts free-stream winds (Figure 3b).

In contrast to locations mantled by sand, exposed sections of the rim are characterized by bedrock possessing numerous fractures that are identified in GPR data as discontinuous reflections within the constituent granitic and granodioritic orthogneisses. Based on information related to impact processes, it is likely that fracturing of the rim rocks occurred during the impact event [e.g., *Wilshire and Moore*, 1974]. During impact, passage of compression and rarefaction waves result in partial comminution of the structurally uplifted rocks contributing to the crater rim [e.g., *Shoemaker*, 1960; *Gault*, 1974; *Wilshire and Moore*, 1974; *Oberbeck*, 1975].

GPR reflections from beneath the sand sheet are also varied but show consistent trends within and around the crater. Short transects (several hundred meters) extending from the exposed rim toward the crater interior trace a reflection beginning at the edge of the finegrained eolian crater fill and descending toward the center of the crater. While the gradient characterizing the surface of the eolian crater fill decreases toward the center of the crater, these GPR data indicate that the gradient along the uppermost portion of the contact between the eolian fill and underlying units matches those on exposed upslope surfaces (after adjusting for changing depth to the alluvium/wall reflection). Examination of surfaces exposed just above the limit of the eolian crater fill confirms that the reflection corresponds to the interior bedrock wall of the crater and/or variably coarse (fragments mostly sand and granule sized) deposits of colluvium/alluvium superposing the bedrock wall.

Transects descending the exterior flank of the crater cross the exposed, fractured rim rocks, which become buried beneath the thickening sand sheet. A distinct reflection first appears between 200 and 300 m from the rim and continues to near the base of the crater flank (Plate 2a), where it becomes discontinuous before dropping into a mostly sand filled topographic swale (visible to the northeast of the crater in Plate 1). Shallow reflections from within the swale are traceable for tens of meters and are comparable to those observed in the eolian sands elsewhere around the crater. Another continuous reflection rises toward the distal edge of the swale (Plate 2b) and continues uninterrupted to the end of the transects.

Analysis of multiple samples from the distinct reflection on the crater flank reveals poorly to very poorly sorted (standard deviation in grain size ranges between 1.1 and 1.6 phi units), subrounded fragments with a modal grain size of 4-8 mm (Figure 4). Pulse travel times in these sediments are close to 7 cm/ns and equate to a dielectric constant of ~16. The granitoid composition of fragments comprising the unit is comparable to that observed in outcrops located higher on the rim. By comparison with textural properties expected for either a pristine ejecta deposit or an accumulation of sediments derived from the rim crest via mass wasting [e.g., see *Grant and Schultz*, 1993a], the sediments within the crater flank unit are relatively well sorted and rounded. Moreover, the coarse character of the bulk of the deposit rules out an origin related to eolian activity. A paucity of radar reflections from within the upper section of the deposit and ground truth from multiple excavations suggest little variation in depositional process during at least the waning stages of emplacement. Collectively, the location and textural properties of the flank deposit are most consistent with those expected for alluvium emplaced as a result of wash and/or limited fluvial transport of material eroded after in situ modification by physical and chemical weathering from higher along the exposed rim.

With one important exception, reflections emerging toward the distal side of the swale at the base of the crater rim and extending for a considerable distance beyond are created by nodular to massive pedogenic calcrete horizons that variably incorporate eolian sands and rare, large (>2-4 mm) granitic fragments. On the northeast side of the crater, the reflection emerging from the distal side of the swale can be traced to outcrops along an erosional escarpment approximately 2 crater radii from the rim crest and confirm that these calcretes directly overlie either older paleodune deposits and/or in situ granitic country rock. Excavations confirm the interpretation of the GPR data, which indicate similar stratigraphic relationships to the east.

An isolated GPR reflection beneath a slightly elevated surface 2.4 crater radii north of the rim is created by an

unusually blocky deposit that covers an area measuring several hundred meters on a side (Plate 3). Dissolution of pedogenic calcrete accumulations binding some fragments and subsequent definition of textural properties demonstrate the fragments comprising the deposit possess a modal size considerably coarser than those examined by sieving (>1.6 cm in diameter, Figure 5), are unsorted (standard deviation in grain size is 2.75 phi units), and angular to subangular. Individual recovered fragments are as large as 9 X 5 X 3 cm and are supported in a finer-grained matrix. Hence the fragments are anomalous because they are coarser, poorly sorted, and more angular than the fragments comprising the deposits excavated on the exterior crater flank, the plains east of the crater flank, and weathering debris shed from outcrops northeast of the crater. Grain mounts made from granitic fragments excavated from within the deposit display abundant planar deformation features in quartz, thereby confirming involvement in the impact event.

The textural properties of the sediments comprising the blocky deposit 2.4 crater radii north of the rim together with an elevated position well beyond the rim base swale indicate emplacement was unrelated to fluvial/alluvial transport from the rim or surrounding plain. Similar arguments can be used to dismiss the possibility that the deposit comprises a debris flow shed off the crater rim. Angularity of the fragments indicates minimal low energy transport: chemical weathering following emplacement and/or low-energy grain impacts during significant transport would yield more rounded fragments resembling those comprising the crater flank alluvium. Instead, the deposit is identified as preserved ejecta that are modified by colluvial and pedogenic processes, but remain largely in situ.

At first glance, preservation of the ejecta on a slightly elevated surface may appear counter intuitive. It may be analogous, however, to the preservation of ejecta on elevated surfaces at comparable range around Meteor Crater [*Grant and Schultz*, 1993a]. At Roter Kamm the elevated position of the preserved ejecta patch would have afforded protection from fluvial/alluvial gradation (except any local surface wash) and contributed to locally improved drainage that would reduce subsequent weathering rates. Instead, the exposed ejecta would have undergone eolian modification that likely contributed to formation of a surface lag of coarse fragments. Subsequent erosion of the ejecta fragments would have been limited by weathering rates and the associated breakdown of the large, initially pristine, fragments to easily transported sizes.

The grain size properties of the ejecta at Roter Kamm are remarkably similar to those at Meteor Crater [*Grant and Schultz*, 1993a] over the range of sizes assessed by sieving. This is in spite of differences in target rocks at the two impact sites (crystalline at Roter Kamm and sedimentary at Meteor Crater) and suggests that grain size properties of at least the fine component of impact ejecta (corresponding to fragments less than ~1 cm in diameter) are largely independent of target rock properties. Moreover, the relative abundance of gravel versus sand versus silt and clay in the Roter Kamm ejecta deposit indicates a high hydraulic conductivity (~30 m/d see [*Summers and Weber*, 1984]). This value is slightly higher than that noted for the ejecta at Meteor Crater (7-9 m/d [*Grant and Schultz*, 1993a]) and implies that preservation/burial of continuous ejecta deposits creates good aquifers with a moderate-to-high reservoir potential. This conclusion is consistent with the discovery of petroleum reserves associated with some buried impact craters [*Koeberl and Anderson*, 1996].

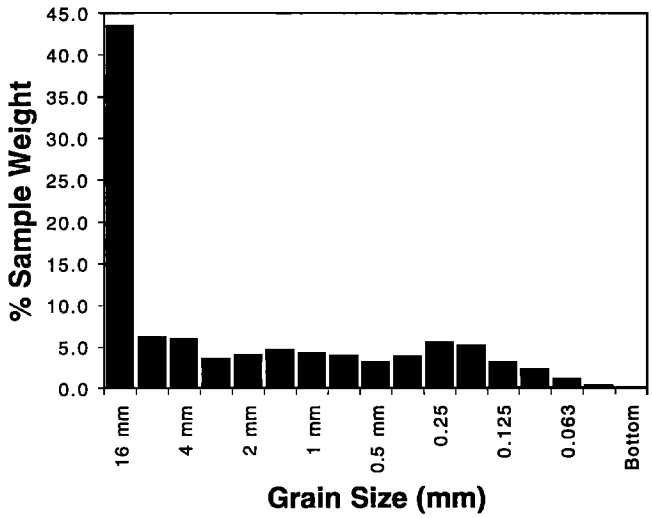

Figure 5. Grain size histogram of the sediment comprising the blocky material on the elevated surface 2.4 crater radii from the crater rim (see Plate 3). The sediments are poorly sorted, subangular, and coarse relative to the crater flank alluvium. Fragments in the deposit possess a modal diameter that is coarser than examined by sieving (>1.6 cm), and individual fragments are up to 9 X 5 X 3 cm. Sample was washed in a ~2 N HCl solution prior to sieving to remove pedogenic carbonate accumulations.

Collectively, the GPR and sedimentologic data described assist in distinguishing deposits at Roter Kamm that preserve at least a partial record of past and ongoing gradation by mostly fluvial/alluvial and eolian processes, Resultant erosion by these processes removed almost all of the continuous ejecta deposit. It is possible that mass wasting deposits occur at the crater, but remain undetected. Mass wasting deposits could be interbedded with the flank alluvium (as debris flows) or occur along the buried portion of the interior wall. The low slope of the interior crater walls and the failure to detect these deposits within the depth range probed by the GPR suggest any mass wasting would have occurred earlier in the history of the crater when higher gradients likely prevailed [e.g., *Roddy*, 1978; *Grieve and Garvin*, 1984; *Garvin et al.*, 1989] or in association with fluvial/alluvial activity (e.g., formation of debris flows). With these points in mind, the juxtaposition of the defined gradational deposits is considered in light of the limited occurrence of ejecta in order to constrain the amount of gradation at the crater.

Discussion

Degradation Processes

Eolian and alluvial processes each played a role in modifying the Roter Kamm impact crater since its formation in 3.7 Ma. Much of the more recent history of crater modification relates to eolian processes. Active mobile sands largely bury the crater and effectively mask most of the signatures associated with prior activity by other processes. Ongoing eolian erosion is responsible for scouring of the exposed rim

that is manifested in the form of numerous, well-formed ventifacts. The amount of eolian stripping, however, is limited by the minimal extent of resistant, mostly granitoid outcrops that remain little altered by chemical weathering.

At Roter Kamm, several factors indicate that fluvial/alluvial activity preceded eolian gradation. First, accumulation of uniform, relatively coarse alluvium along the upper rim (interior and exterior) confirms that runoff and alluvial deposition outpaced both eolian deposition and the rate at which fragments could be further weathered and subjected to eolian stripping. Second, rim relief is punctuated by V-shaped breaches, oriented radial to the crater center, that variably expose bedrock and alluvium/colluvium. The floor of some of these breaches is characterized by gradients of less than 8^0-10^0. These characteristics are most consistent with an origin by incisement and accompanying slope processes, perhaps associated with sections of the rim that were more extensively comminuted during impact. Third, similar gradients occur on the exposed interior wall, alluvium/colluvium mantling slightly lower portions of the wall, and on alluvium/colluvium buried beneath the edge of the eolian crater fill still lower on the wall. Lower gradients should occur on exposed surfaces if significant eolian erosion had followed deposition of the uppermost eolian crater fill.

Consideration of morphology and deposits identified around the crater exterior provides additional evidence for fluvial degradation. First, study of upper rim surfaces and collection of GPR data with supporting samples on lower sections of the rim flank permit delineation of alluvium along every transect that was completed. Although some portions of the exterior flank remain to be explored (e.g., western flank of the crater), the ubiquitous occurrence of alluvium where data were collected, similarities in setting and flank profile between studied versus not studied locations, and analogy with the distribution of alluvium at Meteor Crater imply the crater flank alluvium at Roter Kamm forms a widespread deposit, probably as coalesced fans.

The swale at the base of the crater rim may have been created as a result of interaction between the outward moving crater ejecta and the atmosphere during crater formation [*Schultz*, 1992]. Truncation of flank alluvium by the swale, however, indicates some erosional enlargement of the swale occurred prior to infilling by eolian sediments (Plate 2a and 2b). Transport of relatively coarse (4-8 mm, see Figure 4) flank alluvium during enlargement of the swale is inconsistent with the smaller size of wind-tranported sediment at the crater (0.20-0.25 mm) and rules out eolian activity as the responsible erosional agent. Moreover, the relatively low gradient along the floor of the swale ($<1^0$) argues against erosion by mass wasting. Fluvial erosion is the most likely cause of swale enlargement because any discharge from the crater flank would have collected there. Under this scenario, truncation of the flank alluvium would reflect accumulation of runoff in the swale from around the flank that enabled continued entrainment and transport after local aggradation of the flank alluvium had slowed or ceased. Eventually, diminished precipitation, runoff, and/or the advance of the sand sheet across the region resulted in inactivity and burial of both the flank alluvium and the swale.

Evidence for mass wasting at Roter Kamm is largely absent, with the exception of local colluvial deposits and the role played by local gravity-driven transport in its formation. At Roter Kamm the thickness of the crater fill together with the limited penetration of the GPR precludes definition of buried mass wasting deposits along the interior wall of the crater that might be comparable to mass wasting deposits within some other craters [*Shoemaker and Kieffer*, 1974; *Grant and Schultz*, 1993a, b]. Nevertheless, the absence of such deposits near the surface of the crater fill or interbedded within alluvium outside the crater coupled with the widespread occurrence of alluvium and eolian deposits in and around the crater on low gradient surfaces (Plate 2 and Figure 2) indicate any mass wasting was followed by alluvial and then eolian gradation.

The inability to locate more than an isolated patch of ejecta 2.4 crater radii north of the crater coupled with the rounded, subdued form of the stripped crater rim provide evidence that most of the continuous ejecta deposit has been eroded from around Roter Kamm. Although some areas around the crater remain unexplored, the locations investigated were mostly between the rim and ~2 crater radii from the rim crest and of typical character and relief. Moreover, radar penetration and supporting ground truth were sufficient to confirm that ejecta do not occur along transects extending beyond the swale at the base of the exterior flank. No GPR data were collected on the west side of the crater, but large outcrops of basement granitoids and Gariep marble are present in this area and are stripped of any possible ejecta. Should undetected ejecta still exist, they must be patchy, thin occurrences. For example, it is possible that some additional ejecta are preserved beneath alluvium on the crater flank. Indeed, W.U Reimold et al., 1997 (Suevite from the Roter Kamm impact crater, Namibia, submitted to *Meteoritics and Planetary Science*) recently reported on the first confirmed occurrence of suevite on the west-northwest rim of Roter Kamm. Despite repeated and thorough geological study of all exposures on the crater rim, this isolated patch of suevite remains the only impact ejecta on the rim known to date. The almost complete erosion of ejecta from the crater rim provides support for the conclusion reached in the present paper that the Roter Kamm impact structure experienced significant gradation.

Comparison between the degraded wall and rim morphology at Roter Kamm and that expected for a pristine crater [*Roddy*, 1978; *Grieve and Garvin*, 1984; *Garvin et al.*, 1989] (Figure 2) helps constrain the amount of rim erosion that has occurred. For example, if rim erosion affected only the ~250 m of the interior wall between the point corresponding to the probed limit of the eolian crater fill and the rim crest, then restoring the present wall profile (sloped at 8^0-22^0) to the repose angle (~30^0) requires an increase in rim height of ~40-100 m above the current position of the rim crest. Restoring the present wall profile to 30^0 in the extreme case that rim erosion was accomplished solely by wall backwasting and crater widening of ~10% requires locating the position of the original rim crest ~120 m closer to the crater center and 20-50 m above the crater wall presently exposed at that location. It is unlikely, however, that rim erosion occurred without some downwasting [*Shoemaker and Kieffer*, 1974; *Roddy*, 1978; *Grant and Schultz*, 1993a, b]. Moreover, erosion was probably not limited to the presently exposed ~250 m of the interior wall, and initial wall slopes were probably steeper than the repose angle (see Figure 2 comparison between Meteor Crater and Roter Kamm). Actual rim erosion therefore could be greater than estimated: restoring wall slopes to 30^0 from a point 350 m from the rim requires an increase in rim height of 65-130 m

above the present rim crest and 40-75 m if wall backwasting has resulted in ~10% crater widening.

Some constraint on the reality of these estimates of rim erosion may be obtained from comparison between the ratio of reconstructed rim height (above the level of the surrounding plain) to crater diameter (present rim crest-to-rim crest diameter of 2.5 km) at Roter Kamm and at Meteor Crater. At Roter Kamm, restoring the wall slope to 30^0 from a point 250 m from the present rim requires addition of 40-100 m to the current rim of 40-90 m height (40 m added to areas of highest slope and 100 m added to areas of lowest slope) and results in a rim height of ~130-140 m above the level of the surrounding plain). The resultant rim height to crater diameter ratio is 0.052-0.057, similar to the value of 0.058 (based on values presented by *Roddy*, [1978] derived for the relatively pristine Meteor Crater [*Grant and Schultz*, 1993b]. Hence, a minimum of ~40 m slope sensitive erosion of the rim appears likely at Roter Kamm and is consistent with the range in rim crest relief and nearly complete erosion of ejecta from around the crater. By way of comparison, Roter Kamm is considerably more eroded than the ~220,000 year old Pretoria Saltpan crater, South Africa [*Brandt and Reimold*, 1995], and more eroded than the 0.5-3.0 m.y. old [*Lambert et al.*, 1980] Talemzane crater, Algeria [*Grant and Schultz*, 1993b].

Timing of Degradation

Comparison between the processes responsible for gradation at Roter Kamm, stratigraphic relationships between resultant deposits, and information related to past climate at the crater [*McKee*, 1982; *COHMAP*, 1988; *deMenocal*, 1995] permit placement of crude constraints on the timing and relative importance of gradational activity. Climate evidence suggests that a progression from somewhat wetter conditions to the arid environment of today occurred during climate shifts at about 2.8 Ma, 1.7 Ma, and 1.0 Ma [*deMenocal*, 1995].

Occurrence of alluvium beneath the sand sheet along the crater flank and at least the upper interior wall indicates alluvial processes were once more important than at present. Moreover, the coarse grained nature of the alluvium as compared to the eolian sands demonstrates a greater competence and suggests water-borne transport of fragments resulted in widespread erosion of ejecta prior to onset of arid conditions by about 1.0 Ma and arrival of the regional sand sheet. This statement is supported by occurrence of the sand sheet directly above calcrete and bedrock/paleodune deposits without an intervening deposit and/or lag of coarse ejecta fragments and a paucity of incorporated granitoid fragments in or under the sand sheet that might be derived from removal of the finer fraction of the ejecta. The conclusion that fluvial/alluvial activity associated with somewhat wetter conditions during the first ~1.0-2.7 m.y. history of the crater accounted for much of the gradation at Roter Kamm is consistent with rim relief that was likely produced by incisement.

Eolian gradation dominated modification of the crater during the late Pleistocene and Holocene and was responsible for burial of much of the crater exterior and surrounding plains beneath several meters of sand. Eolian deposition within the crater was more significant and buried all but the upper interior wall beneath an estimated 500 m of fill [*Fudali*, 1973]. The nearly complete burial of the crater severely limits the extent and amount of ongoing eolian erosion. An absence of gullies incising the sand sheet and a paucity of superposing alluvium highlight the minimal role of fluvial/alluvial processes since the onset of eolian deposition: most of the active channels in the vicinity are associated with pediments rising to the east and do not affect the crater.

Possible Implications for Mars

Although preliminary in some respects, the first-order constraints placed on the gradation history of Roter Kamm may help in understanding the gradational evolution of some simple Martian craters [*Grant et al.*, 1996] that experienced early fluvial modification [e.g., *Carr*, 1981, 1995; *Baker*, 1982; *Grant*, 1987; *Craddock and Maxwell*, 1990, 1993; *Fanale et al.*, 1992] followed by eolian degradation [e.g., *Ward*, 1979; *Scott and Tanaka*, 1982; *Arvidson et al.*, 1984; *Christiansen*, 1986; *Schultz and Lutz*, 1988; *Greeley et al.*, 1992; *Grant and Schultz*, 1990, 1993b].

Such comparisons between terrestrial and Martian craters can be valid despite very different timescales over which gradation signatures have evolved and persisted on the two planets. On Mars, gradational activity was likely epochal in nature [*Fanale et al.*, 1992], with long intervening periods of static equilibrium characterized by minimal gradational change [e.g., *Grant and Schultz*, 1990, 1993b]. As described by *Greeley et al.* [1992], current environmental conditions on Mars permit only very limited, mostly eolian gradation across much of the planet. The cumulative effects of such minimal gradation remain small, thereby resulting in minimal modification of pre existing landforms created under alternate conditions. Hence some first-order characteristics of landscapes evolved in the distant past remain preserved and can be evaluated to determine which geomorphic processes contributed to their evolution. Validation of this conclusion occurs in the form of preserved valley networks and other landforms created during the early history of Mars, but whose first-order signatures persist and permit evaluation of processes responsible for their origin [e.g., *Carr*, 1981, 1995; *Baker*, 1982; *Mars Channel Working Group*, 1983].

At Roter Kamm, fluvial/alluvial activity produced a rounded, locally incised rim and reduced interior wall slopes below the repose angle (Figure 2). This activity was accompanied by removal of most continuous ejecta. Similar gradation of Martian craters therefore might be expected to produce broadly comparable characteristics. By contrast, the evolution of rimless simple craters on Mars, whose walls remain sloped near the angle of repose and whose exterior retains recognizable ejecta deposits, apparently involved processes other than, or in addition to, fluvial/alluvial activity (e.g., mass wasting and/or eolian [see *Grant and Schultz*, 1993b]).

Examination of Roter Kamm at the 30 m/pixel resolution afforded by the Landsat thematic mapper (TM) (Figure 1) also provides constraints on the potential for eolian activity to mask signatures created by prior gradation. Arrival and ongoing redistribution of the sand sheet sediments at Roter Kamm form a blanket covering all but the raised rim of the crater. A model for eolian mantling on Mars that calls for uniform burial of all features [*Zimbelman and Greeley*, 1981] may be over simplified therefore because deposition is likely to be accompanied by considerable redistribution of sediments that leave crater rims exposed. On Mars, widespread eolian degradation occurred [e.g., *Ward*, 1979; *Scott and Tanaka*, 1982; *Arvidson et al.*, 1984; *Christiansen*, 1986; *Schultz and*

Lutz, 1988; *Grizzaffi and Schultz*, 1989; *Grant and Schultz*, 1990, 1993b] that post dates activity by alternate processes [e.g., *Zimbelman*, 1987; *Grant and Schultz*, 1990, 1993b]. Analogy with Roter Kamm suggests diagnostic evidence of past gradation in areas modified by eolian mantling may be best exposed along high relief surfaces such as the raised rim of craters.

Conclusions

Use of a GPR at the Roter Kamm impact crater demonstrates the utility of the instrument in helping to define the gradation of a common planetary landform. Although radar penetration in the environment at Roter Kamm was limited to <5 m, it was sufficient to delineate deposits beneath the regional sand sheet, thereby helping to define deposits that record the changing role of gradation processes at the crater. Together with topographic information and sedimentologial analysis of samples taken along transect lines, GPR data indicate that Roter Kamm experienced ~40 m or more of slope sensitive degradation of the raised rim that was accompanied by nearly complete erosion of the continuous ejecta. Only one patch of in situ ejecta deposit was located 2.4 crater radii north of the crater rim. Other ejecta may persist beneath alluvium on the crater flanks or elsewhere around the crater exterior. Any such ejecta remnants are likely of limited extent and thickness, however, based on analysis of GPR data and supporting evidence from outcrops and sampling. Fluvial/alluvial activity likely dominated the first 1.0-2.7 m.y. of gradational activity and was probably responsible for erosion of most of the continuous ejecta deposit. Gradation since the mid-Pleistocene was largely due to eolian activity and led to emplacement of the regional sand sheet.

Finally, results from Roter Kamm may provide some insight into the evolution of degraded Martian craters that experienced possibly analogous fluvial/alluvial gradation followed by eolian modification. By analogy with Roter Kamm, craters on Mars experiencing extended fluvial/alluvial modification would likely display low sloped interior walls and a rounded, but locally deeply incised rim. Rim modification would be accompanied by erosion of most of the continuous ejecta surrounding these craters well before removal of the raised rim. Occurrence of recognizable ejecta around some rimless Martian craters therefore implies gradation by alternate processes.

Acknowledgments. This research was supported by NASA grant NAGW-705 (P.H.S., J.A.G.), the Hochschuljubilaeumsstiftung der Stadt Wien and the Austrian Science Foundation (FWF, project P08794-GEO) (C.K.), Foundation for Research Development, Pretoria, RSA (W U.R.), and the Namibian Geological Survey (all). GPS support was provided by Lutz Wendorff of the Namibian Geological Survey. Dion Brandt, Dona Jalufka, and Yvonne and Carly Reimold provided crucial assistance in the field. Thanks also to Nancy Grant. Comments by two anonymous reviewers resulted in significant improvements to the manuscript.

References

Arvidson, R.E., E.A. Guinness, C Leff, and M Presley, Ancient martian cratered terrain materials exposed by deflation northwest of the Baldet and Antoniadi basins (abstract), *Lunar Planet. Sci., XV*, 19-20, 1984.

Baker, V. R., *The Channels of Mars*, 198 pp., University of Texas Press, Austin, 1982.

Brandt, D., and W.U. Reimold, A structural and petrographic investigation of the Pretoria Saltpan impact structure, *S. Afr. J Geol.*, *98*, 287, 1995.

Carr, M.H., *The Surface of Mars*, 232 pp., Yale University Press, New Haven, Conn., 1981.

Carr, M.H., The Martian drainage system and the origin of valley networks and fretted channels, *J. Geophys. Res.*, *100*, 7479-7507, 1995.

Christiansen, P.R., Regional dust deposits on Mars: Physical properties, age, and history, *J. Geophys. Res* , *91*, 3533-3545, 1986.

Cooperative Holocene Mapping Project (COHMAP) Members, Climatic changes of the last 18,000 years: Observations and model simulations, *Science*, *241*, 1043-1052, 1988.

Craddock, R.A., and T.A. Maxwell, Resurfacing of the Martian highlands in the Amenthes and Tyrrhena region, *J. Geophys. Res.*, *95*, 14,265-14,278, 1990.

Craddock, R.A., and T.A. Maxwell, Geomorphic evolution of the martian highlands through ancient fluvial processes, *J. Geophys. Res* , *98*, 3453-3464, 1993.

deMenocal, P.B., Plio-Pleistocene African climate, *Science*, *270*, 53-59, 1995.

Dietz, R.S., Roter Kamm, Southwest Africa. Probable meteorite crater, *Meteoritics*, *2*, 311-314, 1965.

Doolittle, J.A., Using ground-penetrating radar to increase the quality and efficiency of soil surveys, in *Soil Survey Techniques*, *SSSA Spec. Publ.* vol 20, Soil Sci. Soc. of Am., Madison, Wisc., 1987

Fanale, F.P., S E Postawko, J.B. Pollack, M.H. Carr, and R.O. Pepin, Mars. Epochal climate change and volatile history, in *Mars*, edited by H.H. Kieffer, B.M Jakosky, C.W. Snyder, and M.S. Matthews, pp. 1135-1179, Univ. of Ariz. Press, Tucson, 1992.

Folk, R.L., *Petrology of Sedimentary Rocks*, 185 pp., Austin, Texas, Hemphill, 1980.

Fudali, R.F., Roter Kamm. Evidence for an impact origin, *Meteoritics*, *8*, 245-257, 1973.

Garvin, J.B , J.L. Bufton, B.A. Campbell, and S H. Zisk, Terrain analysis of Meteor Crater ejecta blanket (abstract), *Lunar Planet. Sci., XX*, Lunar and Planetary Institute, Houston, Texas, 333-334, 1989.

Gault, D.E., Impact craters, in *A Primer in Lunar Geology* , edited by R. Greeley and P.H. Schultz, *NASA Tech. Memo., TM-X-62359*, 137-175, 1974.

Gile, L.H., F F. Peterson, and R.B. Grossman, Morphological and genetic sequences of carbonate accumulation in desert soils, *Soil Sci., 101*, 347-360, 1966

Grant, J A , The geomorphic evolution of Eastern Margaritifer Sinus, Mars, Advances in Planetary Geology, *NASA Tech. Memo , 89871*, 1-268, 1987

Grant, J A., and P.H. Schultz, Gradational epochs on Mars· Evidence from west-northwest of Isidis Basin and Electris, *Icarus*, *84*, 166-195, 1990

Grant, J A , and P H Schultz, Erosion of ejecta at Meteor Crater, Arizona, *J Geophys. Res., 98*, 15,033-15,047, 1993a

Grant, J A , and P.H. Schultz, Degradation of selected terrestrial and martian impact craters, *J. Geophys. Res* , *98*, 11,025-11,042, 1993b.

Grant, J A , and P.H Schultz, Erosion of ejecta at Meteor Crater: Constraints from ground penetrating radar, in *Proceedings of the 5th International Conference on Ground Penetrating Radar*, pp. 789-803, Univ. of Waterloo, Ontario, Canada, 1994a

Grant, J.A., and P.H. Schultz, Early fluvial degradation in Terra Tyrrhena, Mars: Constraints from styles of crater degradation on the Earth (abstract), *Lunar Planet. Sci., XXV*, 457-458, 1994b.

Grant, J.A., C. Koeberl, W.U. Reimold, P.H Schultz, D. Brandt, and A J. Franzsen, The degradation history of the Roter Kamm impact crater, Namibia (abstract), *Lunar Planet. Sci., XXVII*, 447-448, 1996.

Greeley, R., N. Lancaster, S. Lee, and P. Thomas, Martian aeolian processes, sediments, and features, in *Mars*, edited by H.H. Kieffer, B.M Jakosky, C.W. Snyder, and M.S. Matthews, pp. 730-766, Univ. of Ariz. Press, Tucson, 1992.

Grieve, R. A. F., and J.B. Garvin, A geometric model for excavation and modification at terrestrial simple impact craters, *J. Geophys. Res.*, *89*, 11,561-11,572, 1984.

Grizzaffi, P , and P.H. Schultz, Isidis Basin: Site of ancient volatile-richdebris layer, *Icarus, 77*, 358-381, 1989.

Koeberl, C., and R R Anderson, Manson and company: Impact structures in the United States, in *The Manson Impact Structure, Iowa: Anatomy of an Impact Crater*, edited by C. Koeberl, and R.R. Anderson, pp. 1-29, Geol. Soc. of Am., Denver, Colo, 1996.

Koeberl, C., K Fredriksson, M. Gotzinger, and W.U. Reimold, Anomalous quartz from the Roter Kamm impact crater, Namibia: Evidence for post-impact hydrothermal activity?, *Geochim. Cosmochim. Acta, 53*, 2113-2118, 1989.

Koeberl, C., J.B. Hartung, M J. Kunk, J. Klein, J.I. Matsuda, K. Nagao, W.U. Reimold, and D. Storzer, The age of the Roter Kamm impact crater, Namibia: Constraints from ^{40}Ar-^{39}Ar, K-Ar, Rb-Sr, fission-track, and ^{10}Be-^{26}Al studies, *Meteoritics*, *28*, 204-212, 1993.

Lambert, P., J.F. McHone Jr., R.S. Dietz, and M. Houfani, Impact and impact-like structures in Algeria, Part I, Four bowl-shaped depressions, *Meteoritics, 15*, 157-179, 1980.

Leeder, M R., *Sedimentology: Process and Product*, 344 pp , George Allen and Unwin, Winchester, Mass , 1982.

Machette, M.N , Calcic soils of the southwestern United States, *Geol Soc. of Am. Spec. Pap., 203*, 21 pp., 1985.

Mars Channel Working Group, Channels and valleys on Mars, *Geol. Soc. Am. Bull., 94*, 1035-1054, 1983.

Matthews, R.K., *Dynamic Stratigraphy*, 370 pp., Prentice-Hall, Englewood Cliffs, N.J., 1974.

McKee, E.D., Sedimentary structures in dunes of the Namib Desert, southwest Africa, *Geol Soc of Am. Spec. Pap., 188*, 64 pp., 1982.

Miller, R M , and W U Reimold, Deformation and shock deformation in rocks from the Roter Kamm crater, SWA/Namibia, *Meteoritics, 21*, 456-458, 1986.

Miller, R M , and K.E.L. Schalk, *Namibia Geological Map*, Geol Surv of Namibia, Windhoek, Namibia, 1980.

Oberbeck, V R., The role of ballistic erosion and sedimentation in lunar stratigraphy, *Rev. Geophys., 13*, 337-362, 1975.

Olhoeft, G.R., Selected bibliography on ground penetrating radar, in *Proceedings of Symposium on Applications of Geophysics in Engineering and Environmental Problems*, Colo. School of Mines, Golden, pp 463-520, 1988.

Pilon, J.A., R A.F. Grieve, and V.L. Sharpton, The subsurface character of Meteor Crater, Arizona, as determined by ground-probing radar, *J Geophys. Res , 96*, 15,563-15,576, 1991

Reimold, W.U., and R. M. Miller, The Roter Kamm impact crater, SWA/Namibia, *Proc. Lunar Planet Sci Conf., 19*, 711-732, 1989

Reimold, W.U , R. M. Miller, R A F Grieve, and C Koeberl, The Roter Kamm impact structure in SWA/Namibia (abstract), in *Lunar Planet. Sci Conf., XIX*, 972-973, 1988.

Reimold, W.U., C. Koeberl, and J. Bishop, Roter Kamm impact crater, Namibia: Geochemistry of basement rocks and breccias, *Geochim. Cosmochim Acta, 58*, 2689-2710, 1994.

Ritter, D F., R.C. Kochel, and J.R. Miller, *Process Geomorphology*, 540 pp., Wm. C. Brown, Dubuque, Iowa, 1995.

Roddy, D.J., Pre-impact geologic conditions, physical properties, energy calculations, meteorite and initial crater dimensions and orientations of joints, faults and walls at Meteor Crater, Arizona, *Proceedings Lunar Planet Sci. Conf., 9*, 3891-3929, 1978

Scholle, P A., and D Spearing, *Sandstone Depositional Environments*, 410 pp., Tulsa, Okla , AAPG Press.

Schultz, P.H., Atmospheric effects on cratering efficiency, *J. Geophys. Res., 97*, 975-1005, 1992

Schultz, P.H , and A.B. Lutz, Polar wandering of Mars, *Icarus, 73*, 91-141, 1988.

Scott, D.H. and K.L. Tanaka, 1982, Ignimbrites of Amazonis Planitia region of Mars, *J. Geophys. Res., 87*, 1179-1190, 1982.

Shoemaker, E.M., Impact mechanics at Meteor Crater, Arizona: 55 pp., Ph.D. dissertation, Geol. Dept., Princeton Univ., Princeton, N.J., 1960

Shoemaker, E.M., and S.E. Kieffer, Guidebook to the geology of Meteor Crater, Arizona, 66 pp., Ariz. State Univ. Cent. for Meteorite Stud., *Publ. 17*, Tempe, 1974.

Summers, W.K. and P.A. Weber, The relationship of grain-size distribution and hydraulic conductivity An alternate approach, *Groundwater, 22*, 474-475, 1984.

Sutton, S R , Thermoluminescence measurements on shock-metamorphosed sandstone and dolomite from Meteor Crater, Arizona, 2, Thermoluminescence age of Meteor Crater, *J. Geophys. Res., 90*, 3690-3700, 1985

Ulriksen, C.P F , *Application of Impulse Radar to Civil Engineering*, Geophys. Surv. Sys., Inc., North Salem, N.H., 175 pp, 1982.

Ward, A.W., Yardangs on Mars: Evidence of recent wind erosion, *J. Geophys. Res., 84*, 8147-8166, 1979

Wilshire, H.G., and H.J Moore, Glass-coated lunar rock fragments, *J. Geol., 82*, 403-417, 1974.

Zimbelman, J., Spatial resolution and the geologic interpretation of Martian morphology: Implications for subsurface volatiles, *Icarus, 71*, 257-267, 1987.

Zimbelman, J and R Greeley, Simulated mantled surfaces on cratered terrain (abstract), *Lunar Planet. Sci., XII*, 1233-1235, 1981.

J. A. Grant, Earth Sciences, SUNY College at Buffalo, 1300 Elmwood Avenue, Buffalo, NY 14222. (e-mail: grantja@snybufaa.cs.snybuf.edu)

C. Koeberl Institute of Geochemistry, University of Vienna, A-1090, Vienna, Austria. (e-mail: a8631dab@vm.univie.ac.at)

W. U. Reimold, Department of Geology, University of the Witwatersrand, Johannesburg 2050, South Africa. (e-mail: 065wur@cosmos.wits.ac.za)

P. H. Schultz, Geological Sciences, Brown University, Box 1846, Providence, RI 02912. (e-mail: peter_schultz@brown.edu)

(Received September 23, 1996; revised March 21, 1997; accepted April 30, 1997.)